# **Hydroelastic Analysis in Frequency Domain and Time Domain**

## \*Frank Lin, Michael Johnson, Zhenhong Wang, and Nigel White

Lloyd's Register Group Ltd

\*Corresponding author: frank.lin@lr.org

#### **Abstract**

Hydroelasticity has been included in ship seakeeping assessment for more than three decades, and it has finally become an essential tool in the marine industry for design of some ship types. In the 35 years of evolution, the hydroelasticity methods applied in the marine and offshore energy industries have grown from two-dimensional to three-dimensional and now feature linear analysis models in the frequency domain and nonlinear models in the time domain. In this paper, we present the three-dimensional hydroelasticity theory model in the frequency domain and time domain, show the difference in the approach, and discuss their applications in wave-structure interaction.

**Keywords:** Hydroelasticity, Springing, Frequency domain, Time domain, Boundary element method, Linear, Nonlinear.

#### Introduction

In the design process for floating structures, like ships and offshore structures, hydrodynamic analysis of wave-structure interaction is the first important step. The methods of rigid-body based seakeeping analysis have been applied successfully in this type of work for many decades, but suffer failures on some of latest mega-ships, like a container ship over 350 meters in length. It has been found that the predicted fatigue life of a large container ship based on a rigid-body approach is significantly longer than when the effects of elastic body responses are taken into account. The elastic-body based analysis method explicitly allows for the interaction of water waves and elastic structures. An ultimate hydroelasticity solution comes from a CFD approach, but this is too expensive to be applied for routine work; for example, the number of required regular wave cases will typically be 3,000 to 5,000 in a design process, and coupled with a few hundred combinations of ship speed, wave headings and sea states, leads to hundreds of thousands of hours of real time simulation. The boundary element hydroelasticity model remains the only tool practical for routine work. In this paper, a general approach for 3D hydroelasticity is presented. Differences between the rigid-body approach and the hydroelasticity approach are discussed. We also look into the theoretical details of the frequency domain hydroelasticity model orientated for conditions of low and moderate sea state, and that of the time domain hydroelasticity model orientated for high sea state conditions.

## Methodology of Hydroelasticity

Accurate prediction of hydrodynamic structural load is key to a successful strength assessment for a structure operated in waves. The hydrodynamic pressure is determined by the location and velocity of the wetted surface of the structure. A rigid-body approach will be accurate enough if the elastic deformation of the structure's wetted surface is small compared to that induced by rigid-body motion. Elastic deformation needs to be considered in the boundary condition of the boundary value problem of flow solution for ships or structures with less stiffness, such as a container ship

longer than 350 meters. The Hydroelasticity Method has been developed for the interaction of waves and elastic structures. Due to the interaction of the flow and the structure's motion and deformation, the hydrodynamic problem and structural dynamic problem is coupled together and needs to be solved simultaneously. Direct finite element structural analysis can be combined with a flow solver like RANS or BEM in time domain to form a robust nonlinear tool for hydroelastic assessment, but it will be too expensive to be practical for routine design assessment. FEM based modal analysis is usually used for the structural assessment portion, and its solution, eigen-values and eigen vectors are used with a boundary element method for hydrodynamic analysis, and this forms the so-called hydroelasticity method for seakeeping analysis. The first 2D frequency domain hydroelastic method was proposed by Bishop and Price in 1979. In their method, a ship was represented by a Timoshenko beam and discretized to a number of 2D beam elements for structural analysis, and the wave flow solution around the ship was determined by strip theory. This hydroelasticity method has continued evolving, now supporting a fully 3D structural FEM model with 3D BEM model for the hydrodynamic solution in both frequency domain and time domain.

In a finite element model of a structure, stress in an element can be estimated by the displacement of the node points of the element. A vector of model node displacements,  $\mathbf{U}$ , can be determined from the model elastic motion equation

$$[\mathbf{M}]\{\dot{\mathbf{U}}\} + [\mathbf{B}]\{\dot{\mathbf{U}}\} + [\mathbf{K}]\{\mathbf{U}\} = \{\mathbf{P}\} + \{\mathbf{F}\} + \{\mathbf{G}\},\tag{1}$$

where [M], [B] and [K] are the matrix of model mass, structural damping and stiffness;  $\{P\}$  is the vector of external surface force;  $\{F\}$  is the vector of external concentrated force, and  $\{G\}$  the vector of external mass force. Dot represents the gradient w.r.t time.

Introducing the homogenous solution of the node displacement vector,  $\{\mathbf{U}\} = \{\mathbf{D}\} e^{-i\omega t}$  and ignoring structural damping and all external forcing terms from equation (1), solution of equation

$$\left(-\omega^{2}[\mathbf{M}]+[\mathbf{K}]\right)\{\mathbf{D}\}=\{\mathbf{0}\},\tag{2}$$

gives the eigen value  $\omega_r$  and eigen vector  $\{\mathbf{D}\}_r$  that define the dry eigenmodes. The number of eigenmodes of a FEA model will be the same as the number of degrees of freedom, being six times of the number of node points. Displacement at point (x, y, z) can be expressed by those dry eigenmodes in terms of summary

$$\{\mathbf{U}(x,y,z;t)\} = [\mathbf{D}(x,y,z)]\{\mathbf{q}(t)\} = \sum_{r} \mathbf{D}_{r}(x,y,z)q_{r}(t)$$
(3)

where  $q_r(t)$  is the amplitude of mode r , the so-called general coordinate, and

$$\{\mathbf{D}\}_{r}^{j} = \left(\mathbf{u}^{r}, \vec{\mathcal{G}}^{r}\right)_{j}^{T} = \left(u_{r}, v_{r}, w_{r}, \alpha_{r}, \beta_{r}, \chi_{r}\right)_{j}^{T}$$

$$(4)$$

is the displacement of point j induced by mode r with unit modal amplitude.

Multiplying  $[\mathbf{D}]^T$  on each term of equation (1), and right multiplying  $[\mathbf{D}]$  on the matrix of model mass, damping and stiffness, we have an equation to determine the modal amplitude

$$[\mathbf{m}]\{\ddot{\mathbf{q}}\} + [\mathbf{b}]\{\dot{\mathbf{q}}\} + [\mathbf{k}]\{\mathbf{q}\} = \{\mathbf{p}\} + \{\mathbf{f}\} + \{\mathbf{g}\},$$
 (5)

One of the advantages of using the dry eigenmode approach is the modal orthogonally. For any elastic dry modes r and s, using Kronecker delta, we have

$$\{\mathbf{D}\}_{r}^{T}[\mathbf{M}]\{\mathbf{D}\}_{s} = \delta_{rs}m_{rs} \quad \text{and} \quad \{\mathbf{D}\}_{r}^{T}[\mathbf{K}]\{\mathbf{D}\}_{s} = \delta_{rs}k_{rs}$$
 (6)

where  $m_{rr}$  and  $k_{rr}$  are the modal mass and modal stiffness.

We can solve the modal amplitude by applying a location and velocity given by equation (3) on the wetted surface in a hydrodynamic analysis model and expressing and estimating the three forcing terms in the hydrodynamic model.

In a boundary element hydrodynamic model, linearized boundary surface condition for unsteady velocity potential  $\Phi^U$  can be given by the surface displacement  $(\mathbf{u}, \vec{\beta})$  and the steady flow velocity  $\mathbf{W}$ 

$$\frac{\partial \Phi^{U}}{\partial n} = \left[ \frac{\partial \mathbf{u}}{\partial t} + \vec{\mathcal{G}} \times \mathbf{W} - (\mathbf{u} \bullet \nabla) \mathbf{W} \right] \bullet \mathbf{n} + O(|\mathbf{u}|^{2}).$$
 (7)

Here **n** is the surface normal vector, and surface displacement  $(\mathbf{u}, \vec{\mathcal{G}})$  can be estimated from the shape functions, or eigen vectors, of the model.

Another fact worth noting in a hydroelastic model is that the eigenmode with nonzero displacement on the wetted surface will receive hydrodynamic pressure force, and we call these modes the "wettable modes". All other modes, "non-wettable modes", have no external force from hydrodynamic pressure. The wettable modes will be coupled to each other through hydrodynamic pressure force, which means the motion of the *i*-th wettable mode will induce a surface forcing term on *j*-th wettable mode. On the other hand, non-wettable modes are uncoupled. In a hydroelastic model, we only need to consider those wettable modes, usually only the first few wettable modes in practice.

Another difference between a rigid structure and an elastic structure is on the location of the center of gravity, COG. The COG of a rigid structure is a point fixed with the structure when it oscillates in waves. On the other hand, the COG is changing due to elastic deformation and not fixed with the elastic structure when it oscillates in waves. This difference leads to a much complicated equation for the rigid body motion mode of the elastic case.

Let's introduce two Cartesian coordinate systems: 1) the body-fixed frame, **HMF**,  $\tilde{o} - \tilde{x}\tilde{y}\tilde{z}$  with  $\tilde{x}$  - axis pointing to the bow,  $\tilde{o} - \tilde{x}\tilde{y}$  coordinate plane lying on the undisturbed water surface when the ship has no oscillations, and  $\tilde{z}$  - axis positive upward; 2) the moving reference frame, **HRF**, o - xyz, which is an inertial frame moving at the constant ship speed U and which is identical with the body-fixed frame if the ship has no oscillations. The coordinates of the body-fixed frame origin,  $\tilde{o}$ , in the reference frame **HMF**, namely  $\vec{\eta} = (\eta_1, \eta_2, \eta_3)$  define the translational motion of the ship, so called **Surge**, **Sway** and **Heave**. Three Euler angles  $(\eta_4, \eta_5, \eta_6)$  between the body-fixed frame  $\tilde{o} - \tilde{x}\tilde{y}\tilde{z}$  and the reference frame o - xyz define the rotational motion of the ship, also referred to as **Roll**, **Pitch** and **Yaw**. Supposing  $\tilde{o} - \tilde{x}\tilde{y}\tilde{z}$  rotates from the position of o - xyz with the angle  $\eta_6$  about

 $\tilde{z}$  -axis first, then the angle  $\eta_s$  about  $\tilde{y}$  -axis, and finally the angle  $\eta_4$  about  $\tilde{x}$  -axis, we will have the relation between  $\tilde{o} - \tilde{x}\tilde{y}\tilde{z}$  and o - xyz as follow

$$\begin{pmatrix} x \\ y \\ z \end{pmatrix} = \begin{pmatrix} \eta_1 \\ \eta_2 \\ \eta_3 \end{pmatrix} + \mathbf{R} \begin{pmatrix} \widetilde{x} \\ \widetilde{y} \\ \widetilde{z} \end{pmatrix}$$
(8)

where  $\mathbf{R}$  is the mapping matrix defined by the three Euler angles.

By setting the origin on the gravitational center of the structure with zero elastic deformation, the equations for rigid body motion modes, translational and rotational, can be given by

$$M \frac{d^{2} \vec{\eta}}{dt^{2}} + \mathbf{R} \sum_{s} \frac{d^{2} \eta_{s}}{dt^{2}} \mathbf{M}_{s} + \mathbf{R} \left\{ \frac{d\mathbf{w}}{dt} \times \left( \sum_{s} \eta_{s} \mathbf{M}_{s} \right) + \mathbf{w} \times \left[ \mathbf{w} \times \left( \sum_{s} \eta_{s} \mathbf{M}_{s} \right) \right] + 2\mathbf{w} \times \left( \sum_{s} \frac{d \eta_{s}}{dt} \mathbf{M}_{s} \right) \right\} = \mathbf{F}$$

$$(9)$$

$$M\left\{\left(\sum_{s} \eta_{s} \tilde{\mathbf{r}}_{s}^{g}\right) \times \frac{d^{2}}{dt^{2}} + \left(\sum_{s} \frac{d\eta_{s}}{dt} \tilde{\mathbf{r}}_{s}^{g}\right) \times \frac{d}{dt} + \mathbf{w} \times \left[\left(\sum_{s} \eta_{s} \tilde{\mathbf{r}}_{s}^{g}\right) \times \frac{d}{dt}\right]\right\} \left[\mathbf{R}^{T}(\bar{\eta})\right] + \mathbf{J}\left(\frac{d\mathbf{w}}{dt}\right) + \mathbf{w} \times \mathbf{J}(\mathbf{w}) + \sum_{s} \frac{d^{2} \eta_{s}}{dt^{2}} \left[\mathbf{J}_{s} + \mathbf{I}_{s} \left(\bar{\mathcal{G}}^{s}\right)\right] = \mathbf{M}$$
(10)

where M and J are the total mass and moment of mass inertia of the structure;  $\eta_s$  the amplitude of the s-th elastic mode;  $\mathbf{w}$  the vector of rotational velocity;  $\tilde{\mathbf{r}}_s^g$ ,  $\mathbf{M}_s$ , and  $\mathbf{J}_s$  are the modal mass center, modal mass vector and modal mass moment of the s-th elastic mode defined by

$$\widetilde{\mathbf{r}}_{s}^{g} = \frac{1}{M} \mathbf{M}_{s}; \quad \mathbf{M}_{s} = \int \left\{ \widetilde{v}^{s} \right\} dm; \quad \mathbf{J}_{s} = \int_{M} \widetilde{\mathbf{r}} \times \widetilde{\mathbf{u}}^{s} dm.$$
(11)

 $\mathbf{I}_s(\vec{\mathcal{G}}^s)$  is the modal moment of mass inertia and represents the effect due to the elastic rotational deformation of the *s*-th elastic mode

$$\mathbf{I}_{s}(\vec{\boldsymbol{\beta}}^{s}) = \begin{pmatrix} \int_{M} \alpha_{s}(\tilde{\mathbf{y}}^{2} + \tilde{\mathbf{z}}^{2})dm & -\int_{M} \beta_{s}\tilde{\mathbf{x}}\tilde{\mathbf{y}}dm & -\int_{M} \chi_{s}\tilde{\mathbf{x}}\tilde{\mathbf{z}}dm \\ -\int_{M} \alpha_{s}\tilde{\mathbf{y}}\tilde{\mathbf{x}}dm & \int_{M} \beta_{s}(\tilde{\mathbf{z}}^{2} + \tilde{\mathbf{x}}^{2})dm & -\int_{M} \chi_{s}\tilde{\mathbf{y}}\tilde{\mathbf{z}}dm \\ -\int_{M} \alpha_{s}\tilde{\mathbf{z}}\tilde{\mathbf{x}}dm & -\int_{M} \beta_{s}\tilde{\mathbf{z}}\tilde{\mathbf{y}}dm & \int_{M} \chi_{s}(\tilde{\mathbf{x}}^{2} + \tilde{\mathbf{y}}^{2})dm \end{pmatrix}$$
(12)

## **Boundary Element Hydroelasticity Method in the Frequency Domain**

In a linearized frequency domain model, the external disturbance, the wave, is assumed "small" and responses induced by this small disturbance follow the time function  $e^{-i\omega_e t}$ . Where the encounter frequency  $\omega_e$  is a function of incident wave frequency  $\omega$ , ship speed U, and wave heading  $\chi$ 

$$\omega_e = \omega - Uk\cos\chi\,,\tag{13}$$

where wave number  $k = \omega^2/g$ , g is the gravitational acceleration, for deep water, and  $\chi = 0^\circ$  represents the following sea, the moving ship and propagating wave have the same direction, and  $\chi = 180^\circ$  represents the head sea condition.

Unsteady flow velocity potential is defined by

$$\Phi^{U}(\mathbf{r};t) = \operatorname{Re}\left\{ae^{-i\omega_{e}t}\left[-i\frac{g}{\omega}(\phi_{I}(\mathbf{r}) + \phi_{D}(\mathbf{r})) - i\omega_{e}\sum_{j=1}^{L}\frac{\xi_{j}}{a}\phi_{j}(\mathbf{r})\right]\right\},\tag{14}$$

where L is the number of system freedoms. L is 6 for the rigid-body model and 6 plus the number of involved elastic eigenmodes of the Hydroelasticity model.  $\eta_j(t) = \text{Re}(\xi_j e^{-i\omega_e t})$  is the displacement of mode j at time t, and  $\xi_j$  is the complex mode amplitude containing information for amplitude and phase. a is the amplitude of the incident wave and its space velocity potential for deep water is given by

$$\phi_I(x, y, z) = e^{kz} \exp\{ik[(\cos \chi)x + (\sin \chi)y]\}. \tag{15}$$

The first responsibility of the hydroelastic model is determination of the diffraction potential  $\phi_D(\mathbf{r})$  and radiation potential  $\phi_j(\mathbf{r})$  for each system freedom. Both diffraction and radiation potential satisfy the Laplace equation  $\nabla^2 \phi(\mathbf{r}) = 0$  and linearized free surface condition

$$\left[g\frac{\partial}{\partial n} + \left(\frac{\partial}{\partial t} + \mathbf{W} \bullet \nabla\right)^2\right] \phi = 0, \quad \text{on calm water surface } z = 0.$$
 (16)

Additionally, the radiation condition requires the diffraction and radiation wave due to the existence of the ship propagating outward. The velocity potential in the fluid domain and on the boundary surface can be estimated by an integration of a singularity distribution on the wetted hull surface  $S_h$ 

 $G(\mathbf{r}_p, \mathbf{r}_q)$  is the Green's function that satisfies the Laplace equation, free surface condition and radiation condition. The strength of singularity  $\sigma$  can be solved from the boundary integral equation

$$\frac{\partial \phi(\mathbf{r}_p)}{\partial n_p} = \alpha(\mathbf{r}_p)\sigma(\mathbf{r}_p) + \iint_{S_h} \sigma(\mathbf{r}_q) \frac{\partial G(\mathbf{r}_p, \mathbf{r}_q)}{\partial n_p} ds_q.$$
(18)

And  $\alpha(\mathbf{r}_p)$  is the interior solid angle of field point  $\mathbf{r}_p$  on the wetted hull surface  $S_h$ . The required surface condition for the diffraction problem is

$$\frac{\partial \phi_D}{\partial n} = -\frac{\partial \phi_I}{\partial n} \tag{19}$$

and for the radiation problem of j-th motion/elastic mode

$$\frac{\partial \phi_j}{\partial n} = n_j + \frac{1}{i\omega_n} m_j \tag{20}$$

Modal normal component  $n_i$ , the so-called n-term, and m-term can be estimated by

$$n_{j} = \mathbf{u}^{j} \bullet \mathbf{n} m_{j} = \left[ \vec{\mathcal{G}}^{j} \times \mathbf{W} - (\mathbf{u}^{j} \bullet \nabla) \mathbf{W} \right] \bullet \mathbf{n}$$
(21)

Hydrodynamic pressure on wetted hull surface comes from Benoulli's equation using velocity potential and its gradient. Its linearized form is of

$$p(\mathbf{r};t) - p_0 = -\rho \left( \frac{\partial \Phi^U}{\partial t} + \mathbf{W} \bullet \nabla \Phi^U \right)$$
 (22)

The hydrodynamic force on mode i can be computed by integration

$$p_i = -\iint_{S_h} n_i \left[ p(\mathbf{r}; t) - p_0 \right] ds \tag{23}$$

After an order analysis of the perturbation expansion of this theoretical approach, this surface modal force can be expressed in terms of modal amplitude

$$p_{i} = \operatorname{Re} \left\{ e^{-i\omega_{e}t} \left[ E_{i} - (i\omega_{e})^{2} \sum_{j=1}^{L} \xi_{j} \left( A_{ij} + \frac{1}{i\omega_{e}} B_{ij} - \frac{1}{\omega_{e}^{2}} C_{ij} \right) \right] \right\}$$

$$(24)$$

and the modal wave exciting force  $E_i$ , modal wave making added-mass and damping coefficient  $A_{ij}$  and  $B_{ij}$  is computed as follows

$$E_{i} = \rho g a \iint_{S_{h}} n_{i} \left[ \frac{\omega_{e}}{\omega} (\phi_{I} + \phi_{D}) + \frac{1}{i\omega} \mathbf{W} \bullet \nabla (\phi_{I} + \phi_{D}) \right] ds$$
 (25)

$$A_{ij} + \frac{B_{ij}}{i\omega_e} = \rho \iint_{S_h} n_i \left[ \phi_j + \frac{1}{i\omega_e} \mathbf{W} \bullet \nabla \phi_j \right] ds$$
 (26)

The modal restoring coefficient  $C_{ij}$  has a similar, but more lengthy, integration formula.

The modal amplitude for a model without concentrated force can then be solved from

$$\sum_{j=1}^{L} \left[ (i\omega_e)^2 (m_{ij} + A_{ij}) + i\omega_e (b_{ij} + B_{ij} + B_{ij}^V) + (k_{ij} + C_{ij}) \right] \xi_j = E_i,$$
(27)

including the linearized equation of rigid body motion

$$M\frac{d^{2}\vec{\eta}}{dt^{2}} + \sum_{s} \frac{d^{2}\eta_{s}}{dt^{2}} \mathbf{M}_{s} = \mathbf{F}$$

$$\mathbf{J} \left( \frac{d\mathbf{w}}{dt} \right) + \sum_{s} \frac{d^{2}\eta_{s}}{dt^{2}} \left[ \mathbf{J}_{s} + \mathbf{I}_{s} \left( \vec{\mathcal{G}}^{s} \right) \right] = \mathbf{M}$$
(28)

These formulae are expressed in a hydrodynamic reference coordinate system. This system is on the calm water surface and moving at the constant speed U toward the ship moving direction. Therefore it is an inertial coordinate system and the dynamic mass modal force is nil, as the existing mass force is gravity and it is a constant in time in this coordinate system. In this deformation/motion equation,  $B_{ij}^V$  is the coefficient of viscous flow induced damping which is important to those modes having small wave making damping, such as roll motion mode. It is possible to involve nonlinear viscous flow damping in the analysis.  $b_{ij}$  is the coefficient of structural modal damping, which is still a challenge for structural engineers to estimate reliably. So far, this coefficient is mainly determined from model tests and/or sea trials.

In most of the available tools, the structural analysis is performed in a ship fixed coordinate system that leads to nonzero mass modal force with two components, one being induced by the inertial acceleration of the rigid body ship motion, and the other coming from the dynamic gravitational acceleration in this ship fixed coordinate system. This mass modal force will excite every non-wettable mode and therefore those modes may need to be involved in structural assessment.

#### **Boundary Element Hydroelasticity Method in Time Domain**

As described in the previous section, the frequency domain hydroelastic BEM model combines linear structural FEA, linear hydrodynamic BEM with linear or nonlinear deformation/motion equations. It is basically a linear Hydroelasticity approach. This frequency domain approach works well for a ship or offshore structure in low and moderate sea conditions, but it becomes unreliable for large wave cases and a nonlinear model is required. For ship or offshore structures in large waves, the dominant nonlinear factors in hydrodynamic problems are the vertical shape change of the hull surface, i.e. the hull flare, and high wave itself. A cheaper and more efficient time domain hydroelastic BEM model could be considered instead of the ultimate CFD model. The time domain BEM model simulates responses in waves by using a retardation function, the response function to an impulse disturbance and carries the memory effects of disturbances in the past. The retardation function in this time domain BEM model can be determined either by time domain Green's function or by the Fourier transformation of hydrodynamic results obtained from frequency domain analysis. Compared to the first approach, the second approach usually takes less computing time and requires much less computer memory and it is the method we will use in this paper. The important difference between the frequency domain hydroelastic BEM model and the time domain model is that the small wave restriction is removed in the time domain model, and it leads to large responses like structural motion/deformation, internal load and so on. The nonlinear terms need to be involved in the computation of motion/deformation equations and internal loads.

One of the main differences from the linearized frequency domain model is that the rigid-body motion mode can have large amplitude, and equation (9) and (10) are adopted. Also in the time domain model, the modal surface force, i.e. the hydrodynamic force, will be determined by

$$F_i = F_i^{rad} + F_i^{dif} + F_i^{FK} + F_i^{rst} + F_i^{others}, \quad i = 1, 2, ..., L$$
 (29)

where subscript i stands for deformation/motion mode;  $F_i^{rad}$  is the radiation force on mode i;  $F_i^{dif}$  is the diffraction force;  $F_i^{FK}$  is the so-called Froude-Krylov force due to incident waves;  $F_i^{rst}$  is the restoring force due to hydrostatic pressure; and  $F_i^{others}$  represents the force due to all other external effects like mooring, viscous damping, tank sloshing, maneuvering, etc. In contrast with the frequency domain model, the maneuvering force on rigid-body motion mode for a ship with forward speed is a mandatory factor in the time domain simulation. Similarly the mooring force or position stationary force for a floating offshore platform is also important.

The radiation force on mode i that is induced by the motion/deformation of the structure is determined by the convolution

$$F_{i}^{rad}(t) = -\sum_{j=1}^{L} \left[ A_{ij}^{\infty} \ddot{\eta}_{j}(t) + B_{ij}^{\infty} \dot{\eta}_{j}(t) + C_{ij}^{\infty} \eta_{j}(t) + \int_{0}^{t} \kappa_{ij}(t-\tau) \dot{\eta}_{j}(\tau) d\tau \right], \quad i = 1, 2, ..., L.$$
 (30)

 $\eta_j(t)$  is the displacement of mode j at time t,  $A_{ij}^{\infty}$ ,  $B_{ij}^{\infty}$  and  $C_{ij}^{\infty}$  is the coefficient of wave making added-mass, damping and restoring force at infinite encounter frequency.  $\kappa_{ij}(t)$  is the retardation function and can be estimated from

$$\kappa_{ij}(\tau) = \frac{2}{\pi} \int_{0}^{\infty} \left[ A_{ij}^{\infty} - A_{ij}(\omega_{e}) \right] \frac{\sin(\omega_{e}\tau)}{\omega_{e}} d\omega_{e} \quad \text{or} \quad \kappa_{ij}(\tau) = \frac{2}{\pi} \int_{0}^{\infty} \left[ B_{ij}(\omega_{e}) - B_{ij}^{\infty} \right] \cos(\omega_{e}\tau) d\omega_{e}$$
(31)

The diffraction modal force can be expressed in a similar way

$$F_i^{dif} = \int_{-\infty}^{\infty} \kappa_i^D (t - \tau) \zeta_0(\tau) d\tau , \qquad (32)$$

and

$$\kappa_i^D(t) = \frac{1}{2\pi} \int_{-\infty}^{\infty} \left[ \text{Re} \left\{ E_i^D(\omega_e) \right\} \cos(\omega_e t) + \text{Im} \left\{ E_i^D(\omega_e) \right\} \sin(\omega_e t) \right] d\omega_e$$
 (33)

Accuracy of the retardation function for radiation and diffraction modal force will directly affect the analysis results and development of a reliable algorithm for the infinite integration is one of the challenges in this time domain model.

In time domain hydroelastic BEM model, nonlinear rigid body motion equations, (9) and (10), are applied. The nonlinear terms in modal force computation needs to be consistently involved as well.

## **Examples of Application**

Two hydroelasticity codes have been developed in Lloyd's Register, HydroE-FD for the frequency domain model and HydroE-TD for the time domain model. The results of frequency domain hydroelastic analysis are compared against the results of Lloyd's Register's rigid body frequency domain code WAVELOAD-FD. The structural analysis was performed by using Lloyd's Register's FEA code, Trident.

## Example 1 - Linear frequency domain hydroelasticity

A container ship was selected as an analysis example. Particulars of this vessel, including ship dimensions, draft at fore and aft perpendicular, displacement, COG and radii of gyrations, are shown in Table 1. The full ship global FEA model and hydroelastic panel model are shown in Figure 1. A one meter sized panel model was selected to capture the responses in the high wave frequency range. Figure 2 and 3 plot the shape of first 10 wettable elastic dry eigenmodes and their *n*-term. The *n*-term of rigid motion mode roll and pitch are also presented in Figure 3. It can be observed that modes 9, 21 and 28 are the first three vertical bending modes, all the other modes are horizontal modes representing bending, torque or their combinations.

**Table 1: Particulars of container ship model** 

Lbp (m)	325.0
B (m)	43.8
T_fp ( <i>m</i> )	11.075
T_ap (m)	11.405
Displacement (m <sup>3</sup> )	94428
Wetted hull area $(m^2)$	14910
LOG (m)	154.5
VOG (m)	15.342
Kxx (m)	16.088
Kyy ( m )	78.235
Kzz ( <i>m</i> )	78.343
Kxz (m)	6.112

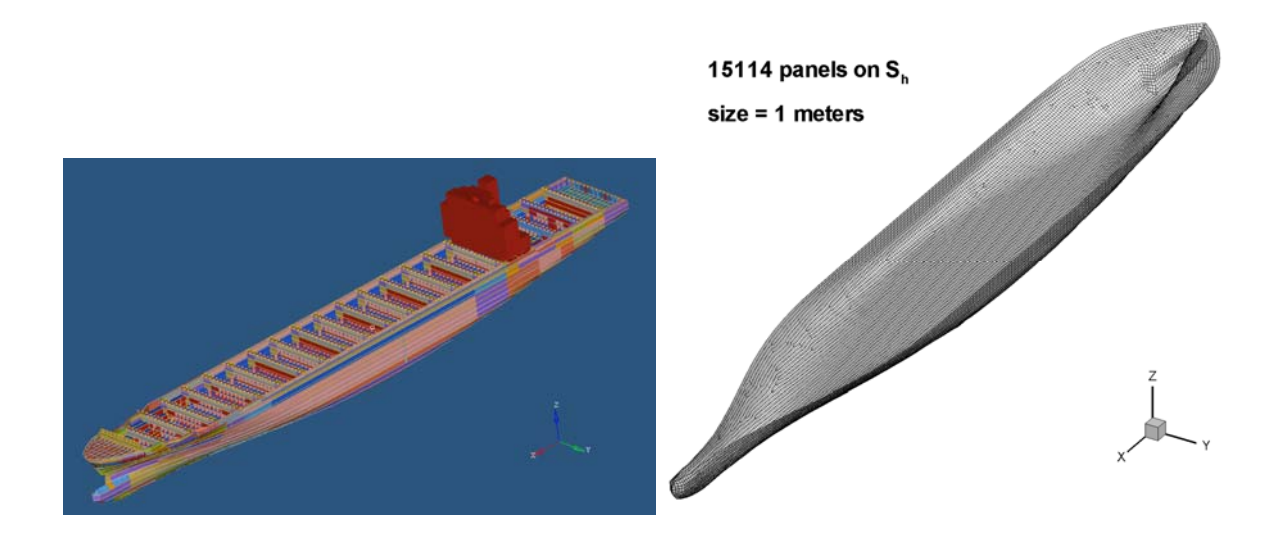


Figure 1: FEA model (left) and hydroelastic panel model (right) of the container vessel.

Figure 4 shows the first key result, being the comparison of the vessel deformation due to the hydrostatic pressure and gravitational force when the vessel is floating in calm water. The upper plot is the result by a direct static 3D FEM analysis and the lower one is the result by HydroE-FD using the modal pressure force due to the hydrostatic pressure and modal mass force due the gravitation. Static modal amplitudes from HydroE-FD are given in Table 2. The main contribution to the static deformation was from the three vertical bending modes as the model is very close to a symmetric case. The ship is in a static hogging state and maximum static deformation by direct FEA using Trident was 324 mm while that from HydroE-FD was 323 mm, so they correlate very well.

Table 2: Static mode amplitude by Hydro-FD

Mode	07	08	09	10	19	20	21	27	28	31
$\xi_j^S$	7.975	11.30	-101.0	0.2505	-0.1286	1.077	-39.87	-0.689	25.46	-0.03120

The natural frequency of each elastic eigenmode is one of most important results in a structural assessment and the results of the "dry natural frequency" and "wave making natural frequency" are listed in Table 3. The "dry natural frequency" represents the natural frequency when the structure oscillates in air or "in vacuum" and these are the eigen values calculated by the whole ship FEA. The "wave making natural frequency" is the natural frequency when the structure oscillates in water and generates the so-called radiation waves. The restoring force and encounter frequency dependent wave making added-mass are considered together with the modal mass and stiffness. From the results, we can see that the wave making effect always decreases the natural frequency and it can even change the sequence of some eigenmodes. In this example, the first vertical bending mode is the third elastic eigenmode (09) in the original dry eigenmode list, but it jumps up to the second elastic mode in the wave making list due to the significant increase of mass due to the wave making added-mass associated with this modal shape. For ocean waves, the typical wave period is on the order of 10 seconds and in general waves of this period do not directly excite resonant oscillation for those eigenmodes with a wave making frequency higher than 5 rad/sec. Waves with higher frequency (> 2 rad/sec) can excite eigenmodes of natural frequency larger than 5 rad/sec. But those shorter waves have smaller amplitude and are usually ignored in many analyses.

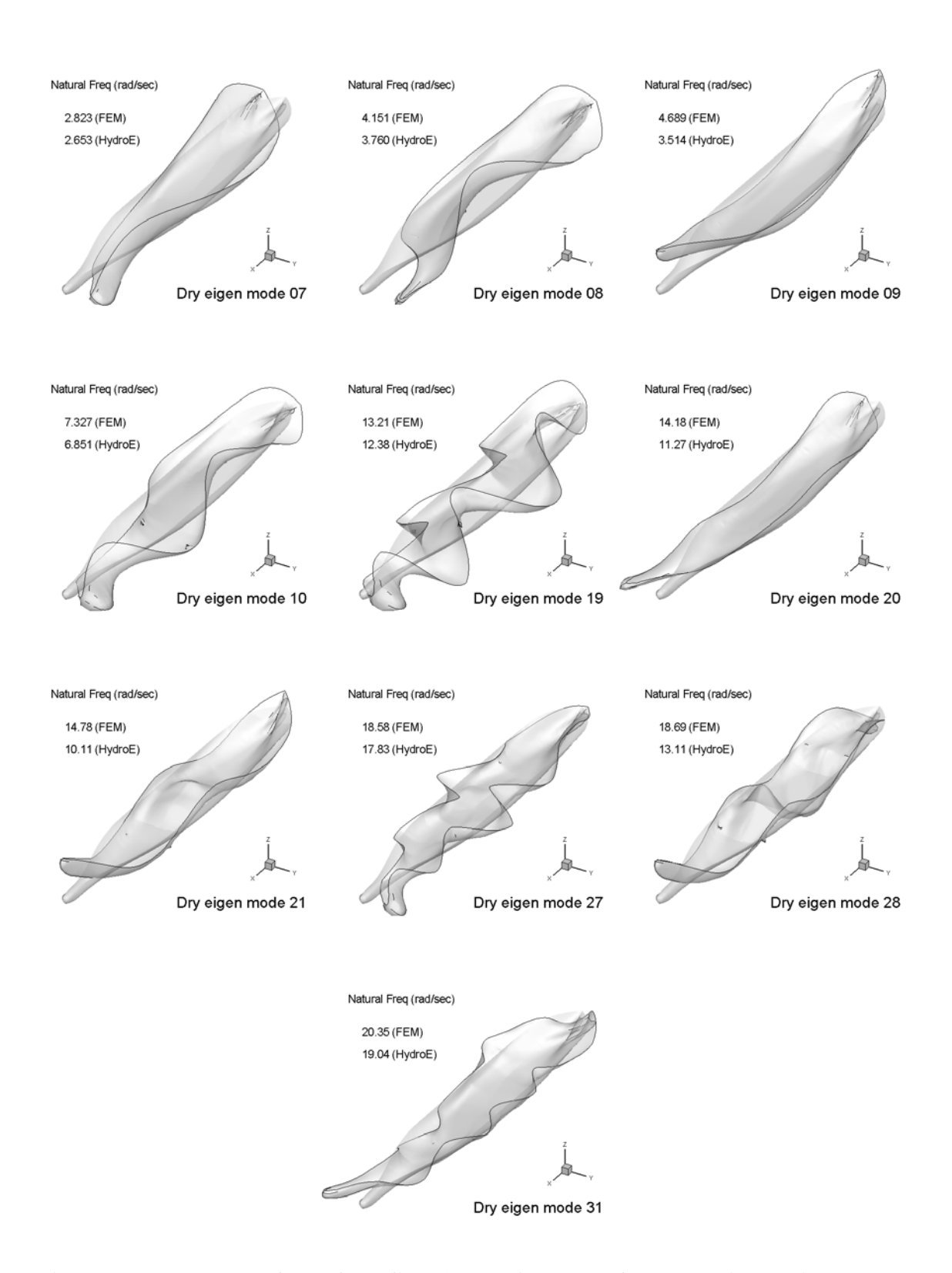


Figure 2: Wetted surface of the first 10 elastic mode of the container ship model.

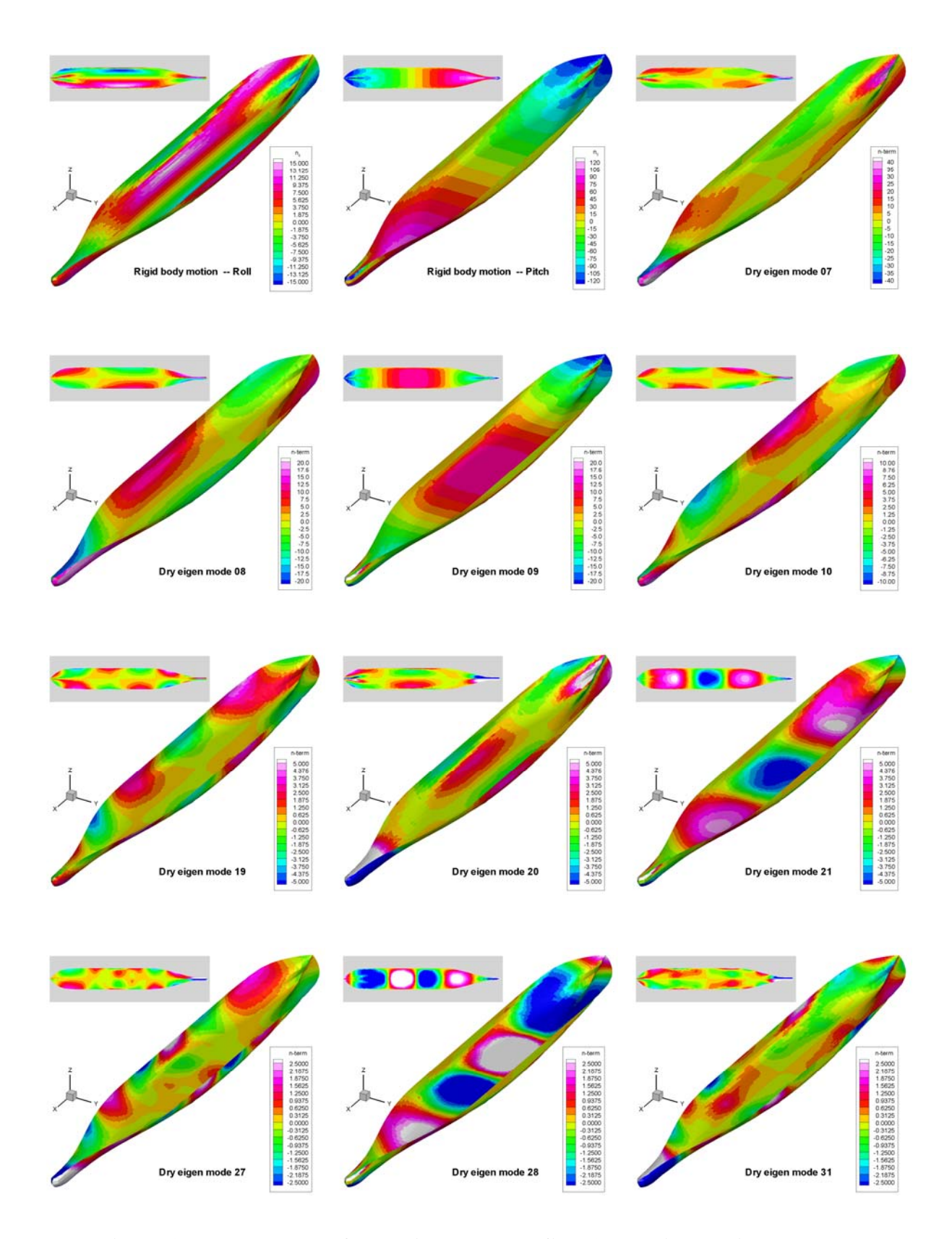


Figure 3: The n-term of roll, pitch, and the first 10 elastic dry eigenmodes.

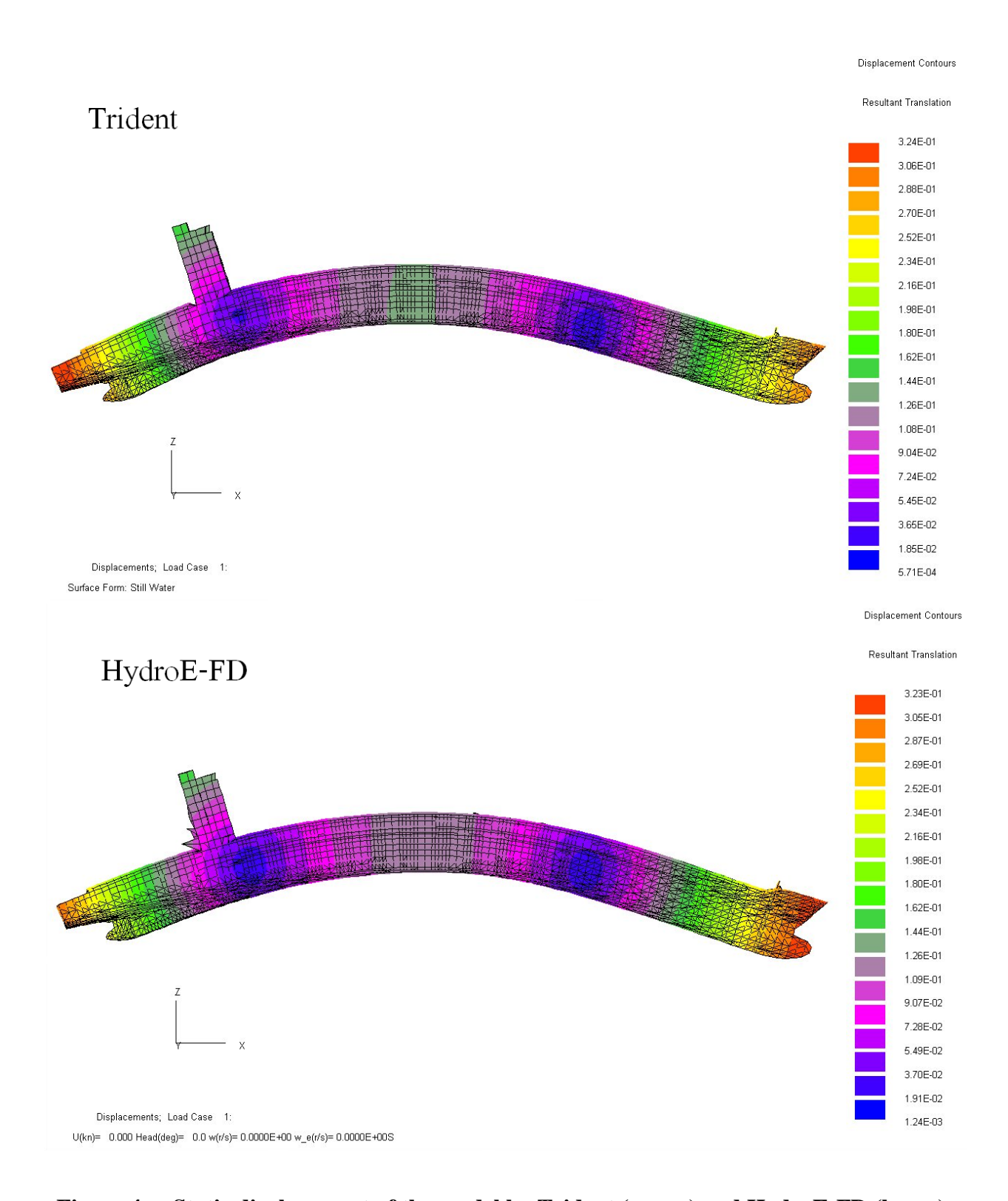


Figure 4: Static displacement of the model by Trident (upper) and HydroE-FD (lower).

**Table 3: Natural frequency of the container ship** 

Eigen	Dry natural frequency	Wave making natural
Mode	from FEA	frequency from
	(rad/sec)	HydroE-FD (rad/sec)
07	2.823	2.655
08	4.151	3.754
09	4.689	<u>3.501</u>
10	7.327	6.851
19	13.21	12.38
20	14.18	<u>11.27</u>
21	14.78	<u>10.11</u>
27	18.58	17.83
28	18.69	<u>13.11</u>
31	20.35	19.04

Table 4: Rayleigh coefficients of structural modal damping for S8100R model

Mode	07	08	09	10	19	20	21	27	28	31
%	1.27	3.29	2.28	1.15	0.67	14.3	1.13	0.0	2.82	0.0

Structural modal damping applied in this example is listed in Table 4.

RAO curves (Response Amplitude Operator curves which represent the response amplitude induced by a wave of 1 meters amplitude) of rigid-body motion (modes 1 to 6) and elastic deformation (modes 7 to N) over a range of incident wave frequency 0.0 to 1.2 rad/sec and 150 degree heading at three ship speeds are plotted in Figure 5. The modal amplitude of the elastic eigenmodes over a wave frequency range 0 to 5 rad/sec at the same ship speed and heading are shown in Figure 6, and the resonant responses of modes 7, 8 and 9 can be found.

Distribution of hydrodynamic pressure RAO is shown in Figure 7 in a resonant condition of the 3<sup>rd</sup> elastic eigenmode, the first vertical bending mode. Compared to the rigid-body analysis results, hydroelastic analysis received much higher pressure in this case. Note the n-term pattern shown in Figure 3, from this we can find that the pattern of the pressure distribution is similar to that of the n-term of the resonant eigenmode, and the radiation pressure is the dominant component in this case.

The modal resonant is determined by two factors, frequency and strength of external excitation. For the case of a ship, an elastic structural eigenmode can be excited when the incident wave has an encounter frequency close to its modal natural frequency. The scale of this resonant eigen response is determined strongly by the pattern of external exciting pressure, including pressure of incident waves and diffraction waves as well as the radiation waves of other modes. The third elastic eigenmode, the 1<sup>st</sup> vertical bending mode, has a resonant amplitude around 6.5 for the zero speed case at a wave frequency of 3.5 rad/sec where the incident wave length is very short, around 5 meters; see Figure 6, top graph. When the wave length increases to 28 meters in 20 the knots case, a

wave frequency of 1.5 rad/sec, the amplitude of this eigenmode jumps up to a level of 50 times larger than that of zero ship speed.

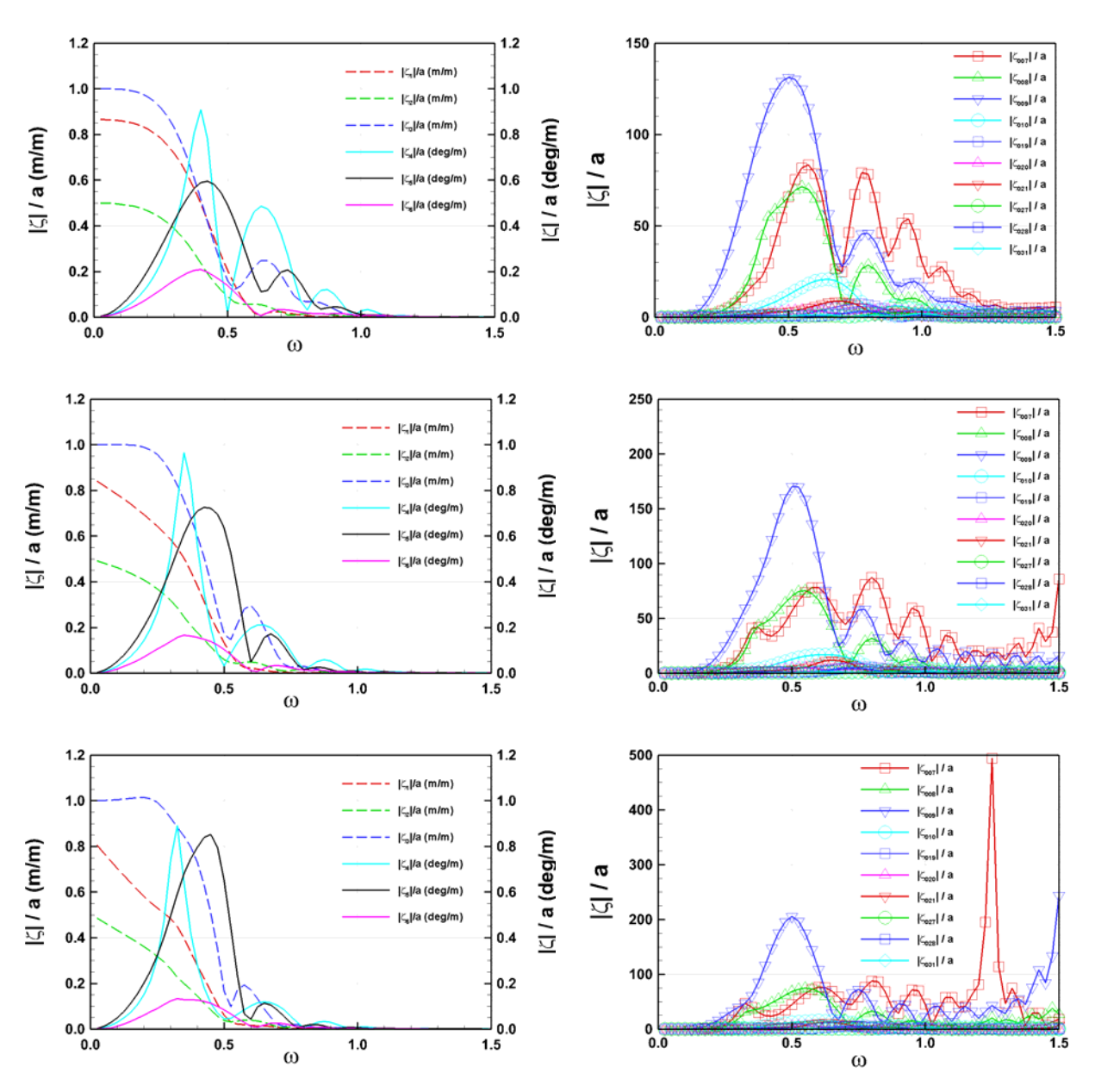


Figure 5: RAO of rigid-body motion and elastic deformation in waves of  $\chi=150^\circ$   $1^{st}$  row: U= 0 knots;  $2^{nd}$  row: U= 10 knots,  $3^{rd}$  row: U= 20 knots  $1^{st}$  column: rigid body motion modes;  $2^{nd}$  column: elastic deformation modes.

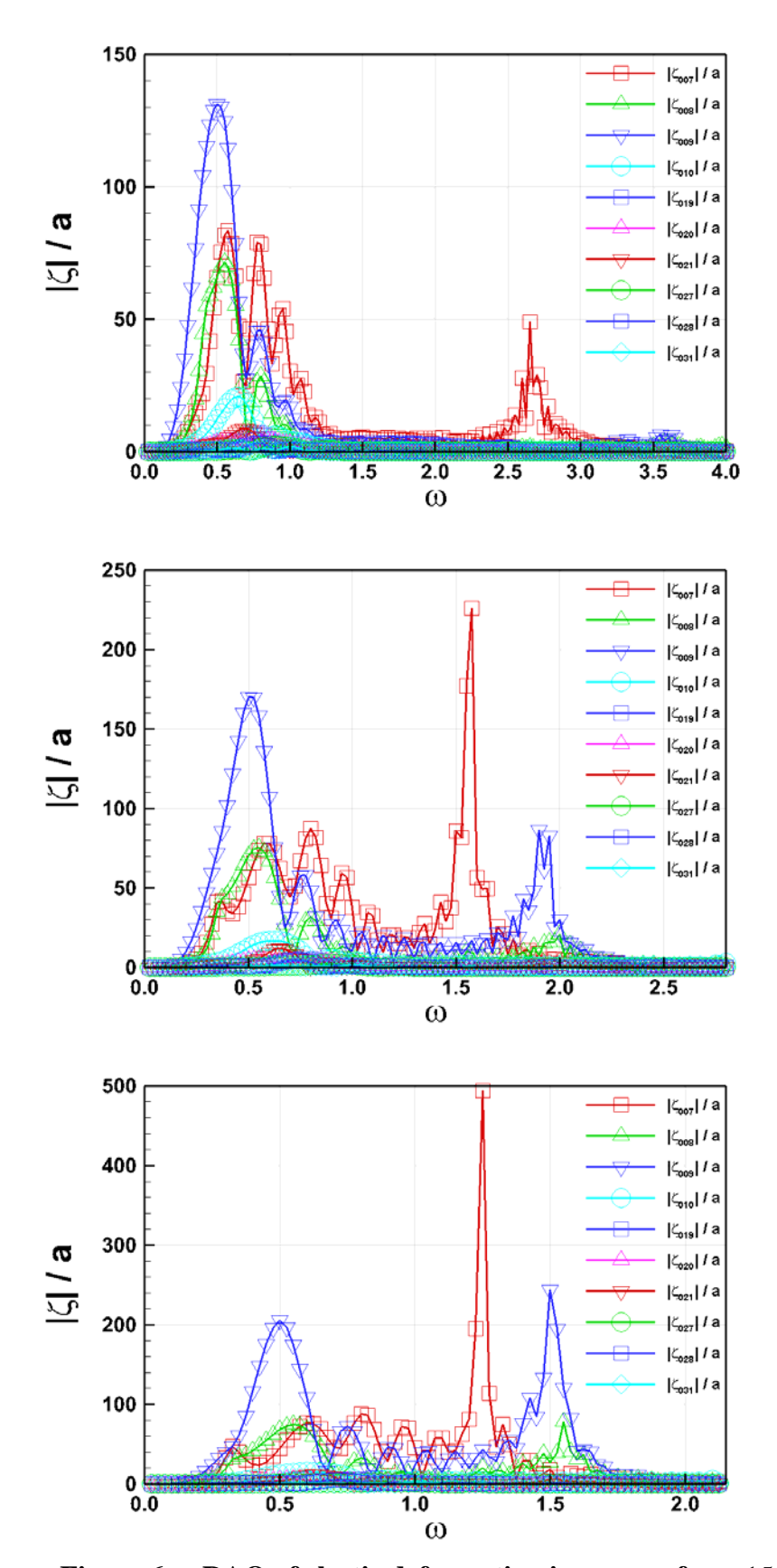


Figure 6: RAO of elastic deformation in waves of  $\chi=150^{\circ}$ 1<sup>st</sup> column: U=0 knots; 2<sup>nd</sup> column: U=10 knots; 3<sup>rd</sup> column: U=20 knots

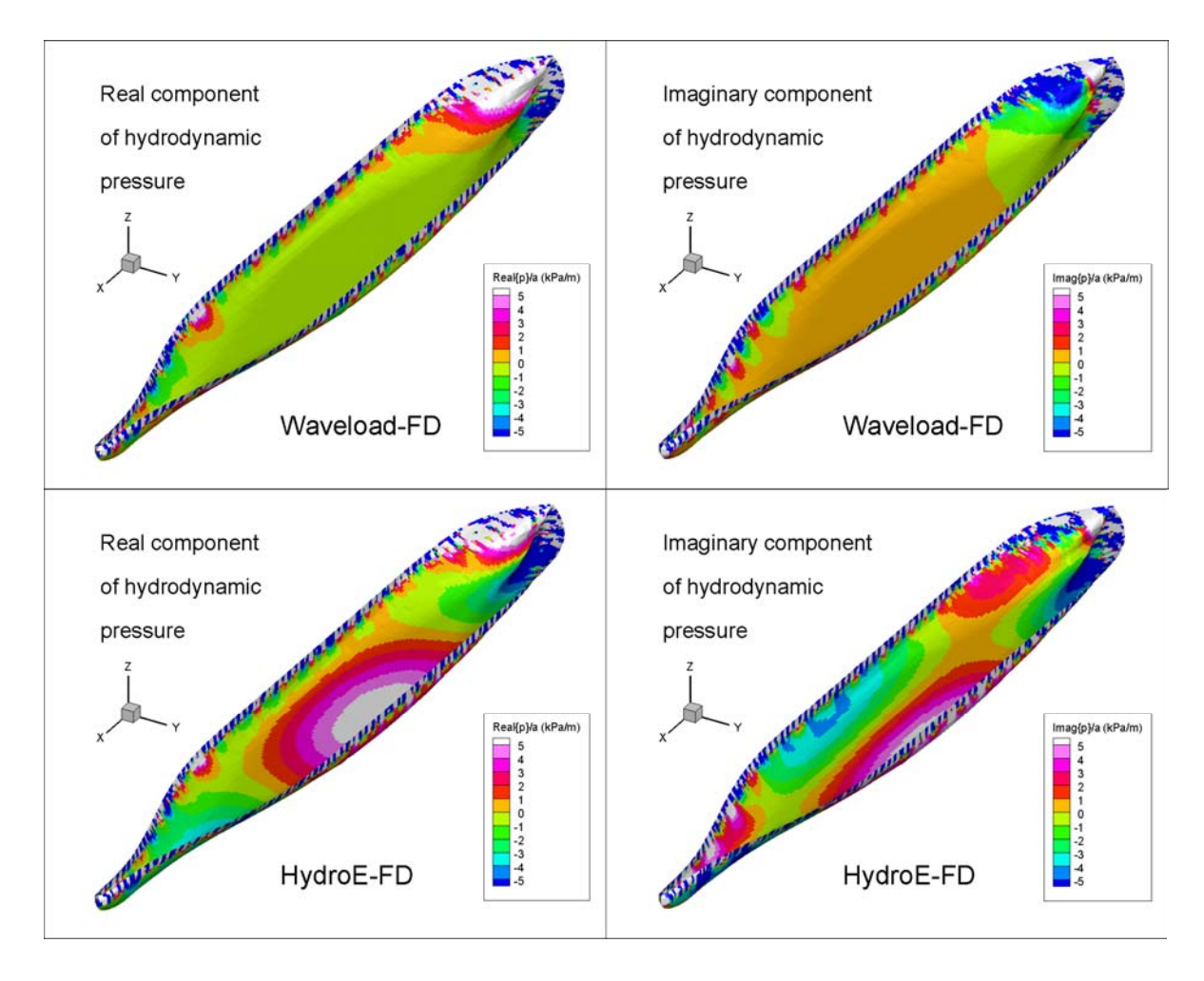


Figure 7: RAO of hydrodynamic pressure of rigid body model (upper) and hydroelasticity model (lower) for condition  $U=12\,\mathrm{knots}$ ,  $\chi=150^\circ$  and  $\omega=1.875\,\mathrm{rad/s}$ .

The internal load values, shear forces, bending moments and torsional moments, are obtained by summation the hydrodynamic pressure and ship motion inertial loads. To check the effects of elastic deformation, internal load results of tension force, horizontal shear force and vertical shear force on a section at 25% of ship length from aft perpendicular are shown on the left column of Figure 8. The torque, vertical bending moment and horizontal bending moment on the mid-ship section are shown in the right column of Figure 8. Blue lines show the results of the frequency domain hydroelasticity model and the results from a rigid-body hydrodynamic analysis are shown as red diamond marks. From this figure, we can see that the internal loads calculated by a hydroelastic analysis method will be close to the results from a rigid-body analysis method when the ship is in waves with encounter frequencies well away from its structural natural frequencies. When the ship is in waves with encounter frequencies close to the structural natural frequencies, then significant feedback can be expected from the internal loads and those resonant internal loads will induce structural vibration, so-called springing, which ultimately may lead to early onset of damage to the ship structure. For curtain types of ship or floating structures, the fatigue life on some structural components based on hydroelasticity assessment can be more than 50% shorter than that by a rigidbody based analysis. A hydroelastic assessment will definitely be required for such cases.

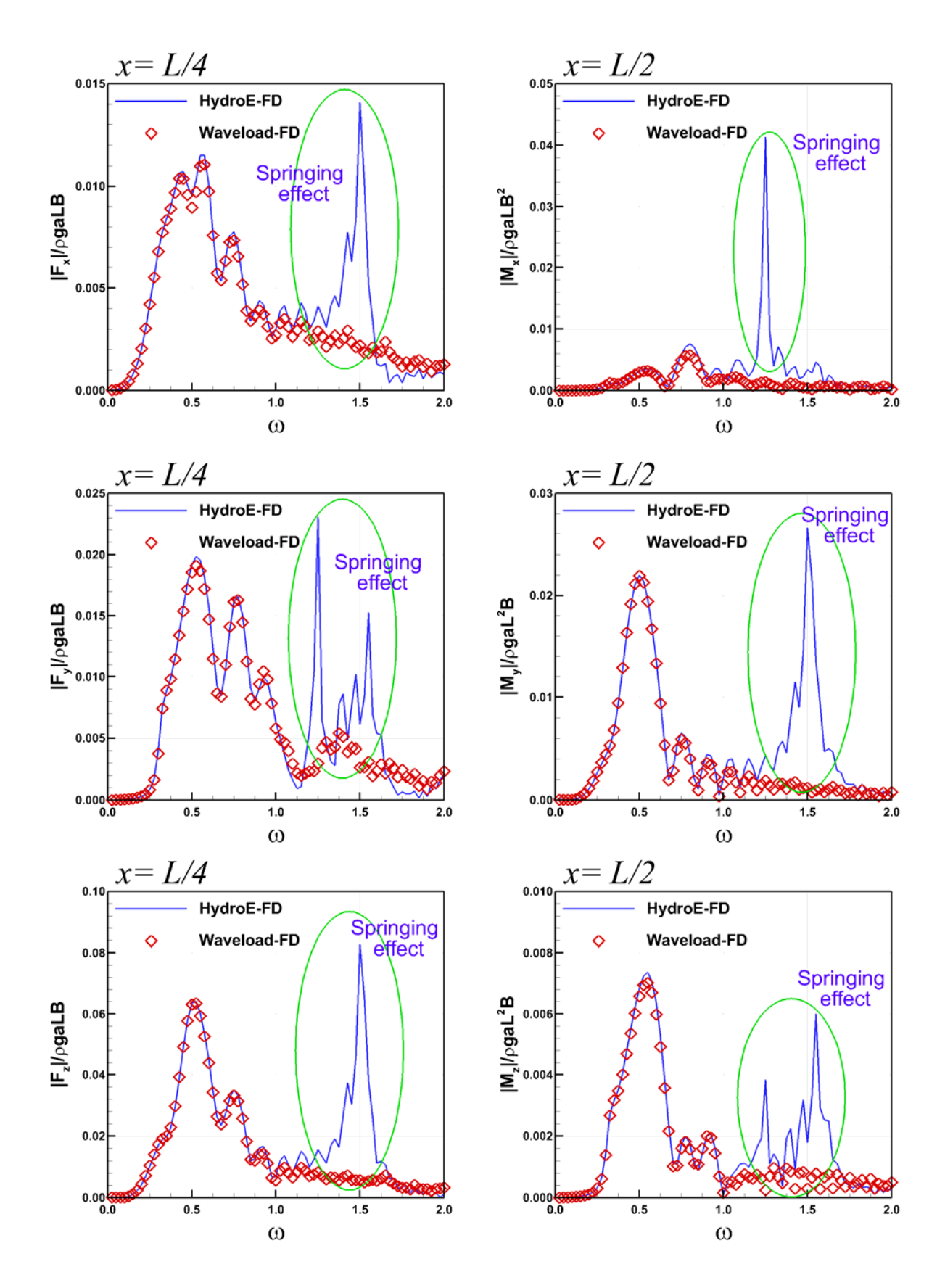


Figure 8: Non-dimensional RAO of internal load in condition of U=20 knots and  $\chi = 150^{\circ}$ .

## Example 2 - Nonlinear time domain hydroelasticity

From analyses of frequency domain hydroelastic results, one can see the reasons for considering hydroelasticity and what impact a hydroelasticity analysis can have on an engineering assessment. We should bear in mind that the frequency domain hydroelasticity is based on a "linear response" condition and works well for cases of waves with small wave steepness. A time domain hydroelasticity model needs to be considered for large wave cases.

We present some results of time domain hydroelasticity analysis for the same ship model below. Time trace of four rigid-body motion modes is shown in Figure 10, for a case in waves of 120 degree heading, 0.375 rad/sec of frequency, 20 meter wave height and ship speed of 10 knots. We can see the time domain model predicts larger motion and nonlinear characteristics for pitch in this extremely high wave condition. The differences in results from the frequency domain analysis and time domain analysis are caused mainly by the so-called geometry nonlinear problem, i.e. the effect of "flare bow" and "flat stern" for the present model above the mean waterline and the lack of buoyancy at both ends below the mean waterline. The frequency domain model and time domain will have similar responses if the wettable surface of the structure has a purely vertical shape, but this is not the case for most ships. Another reason for this difference is the large nonlinear rotation motions. For example, the roll motion amplitude of the present case goes up to 20 degrees, and this roll motion will affect the yaw motion. The effects of roll on yaw in the nonlinear rotation term  $\mathbf{w} \times \mathbf{J}(\mathbf{w})$  and mapping matrix  $\mathbf{R}$  are ignored in a frequency domain model therefore coupling between rotation motions are weaker there.

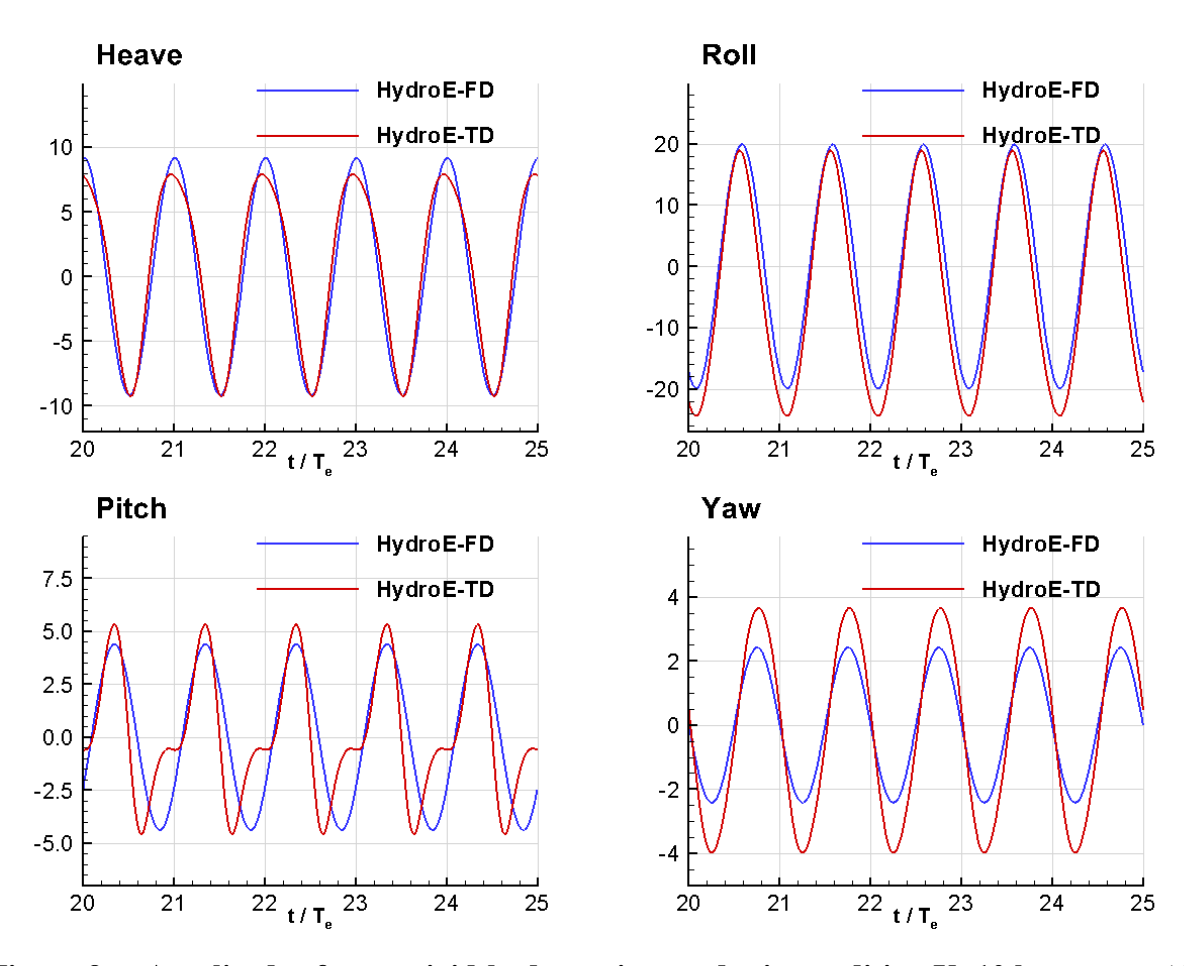


Figure 9: Amplitude of some rigid-body motion modes in condition U=10 knots,  $\chi = 120^{\circ}$ ,  $\omega = 0.375$  rad/sec and wave height = 20 meters.

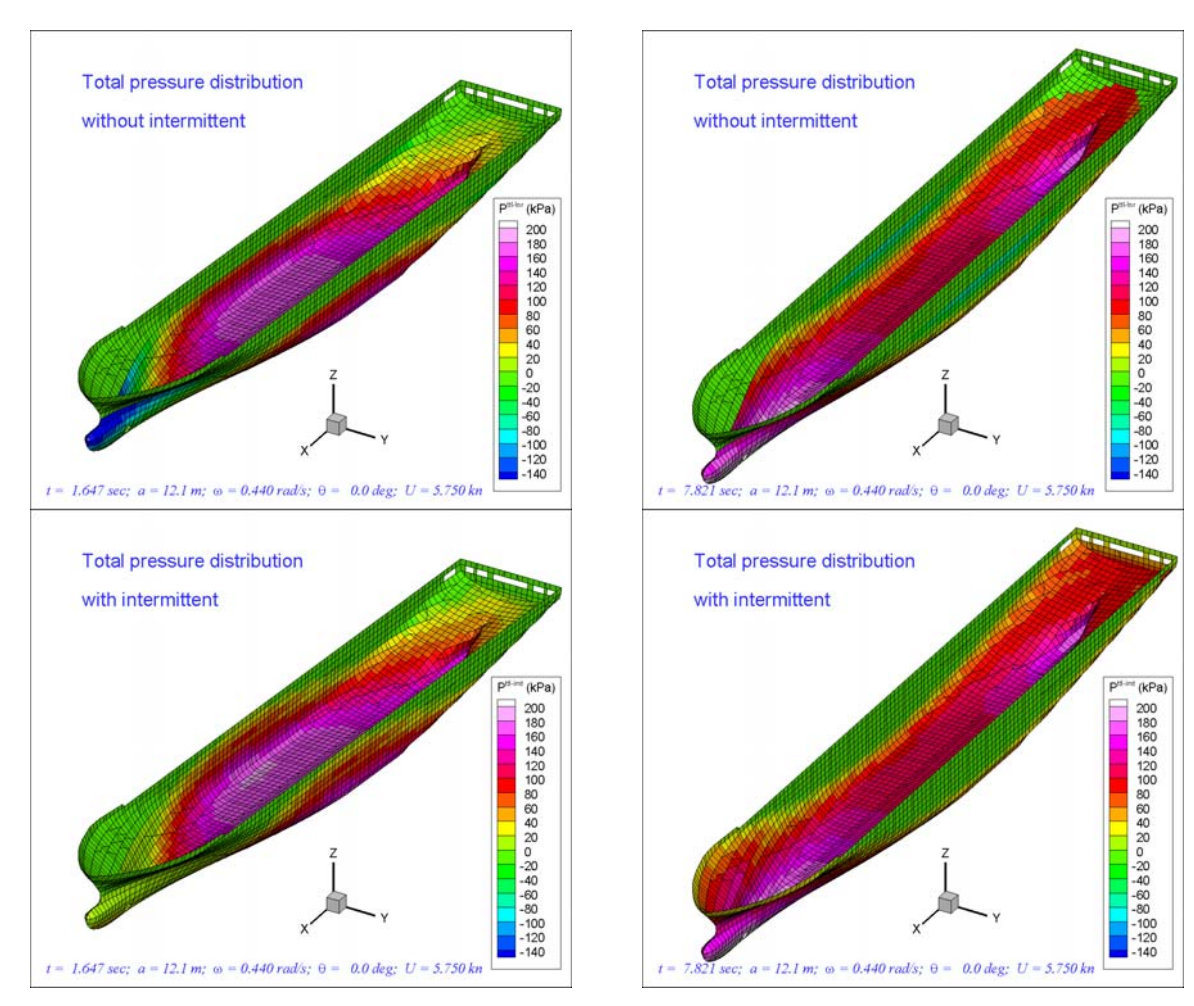


Figure 10: Pressure distribution by frequency domain model (top) and time domain model (bottom) in condition U=5.75 knots,  $\chi=0^{\circ}$ ,  $\omega=0.44$  rad/sec and wave height = 24.2 meters, in a hogging state (left) and a sagging state (right)

The most obvious difference between the frequency domain and the time domain approaches is the pressure distribution, as illustrated in Figure 10. The hydrodynamic pressure only acts on the mean wetted surface of the ship in the frequency domain mode and changes in a pure sinusoidal style. From the top row of Figure 10, labelled "Total pressure distribution without intermittent," showing the linear frequency domain results with the addition of the hydrostatic pressure, we can see that there is no pressure on the mean dry hull surface and the total pressure on the bow can have a negative value in a frequency domain model. On the other hand, the total combined hydrostatic and hydrodynamic pressure calculated by a time domain model has no such problem and the pressure distribution looks much closer to reality, as shown in the bottom row of Figure 10 labelled "Total pressure distribution with intermittent".

A problem in the frequency domain model is the "symmetric vertical load". The magnitude of the dynamic vertical bending moment and shear force will be the same for both the hogging and sagging conditions, but this is clearly not the case due to "intermittent" pressure effects which can become significant for higher waves. For a conventional ship, the dynamic vertical load in a sagging wave condition is normally always larger than in a hogging wave condition. In a time domain model we simulate the instantaneous wetted surface and solve the pressure on this surface, and as a consequence the vertical loads become much closer to reality. The dynamic and total

vertical shear force on a section at ¼ of ship length are presented in the top row of Figure 11, and those for the vertical bending moment on a mid-ship section are presented in the bottom row. This shows that for this example, the dynamic vertical bending moment in the sagging wave case is about twice of that of the hogging wave case. The vertical shear force has similar tendency. It is worth noting that the results of this extreme wave case are for demonstration of the difference of the frequency and time domain models, and we would not expect the ship to be operated at 20 knots in a 20 meters wave environment. The asymmetric ratio of vertical load in sagging/hogging condition will decrease as the wave height becomes smaller.

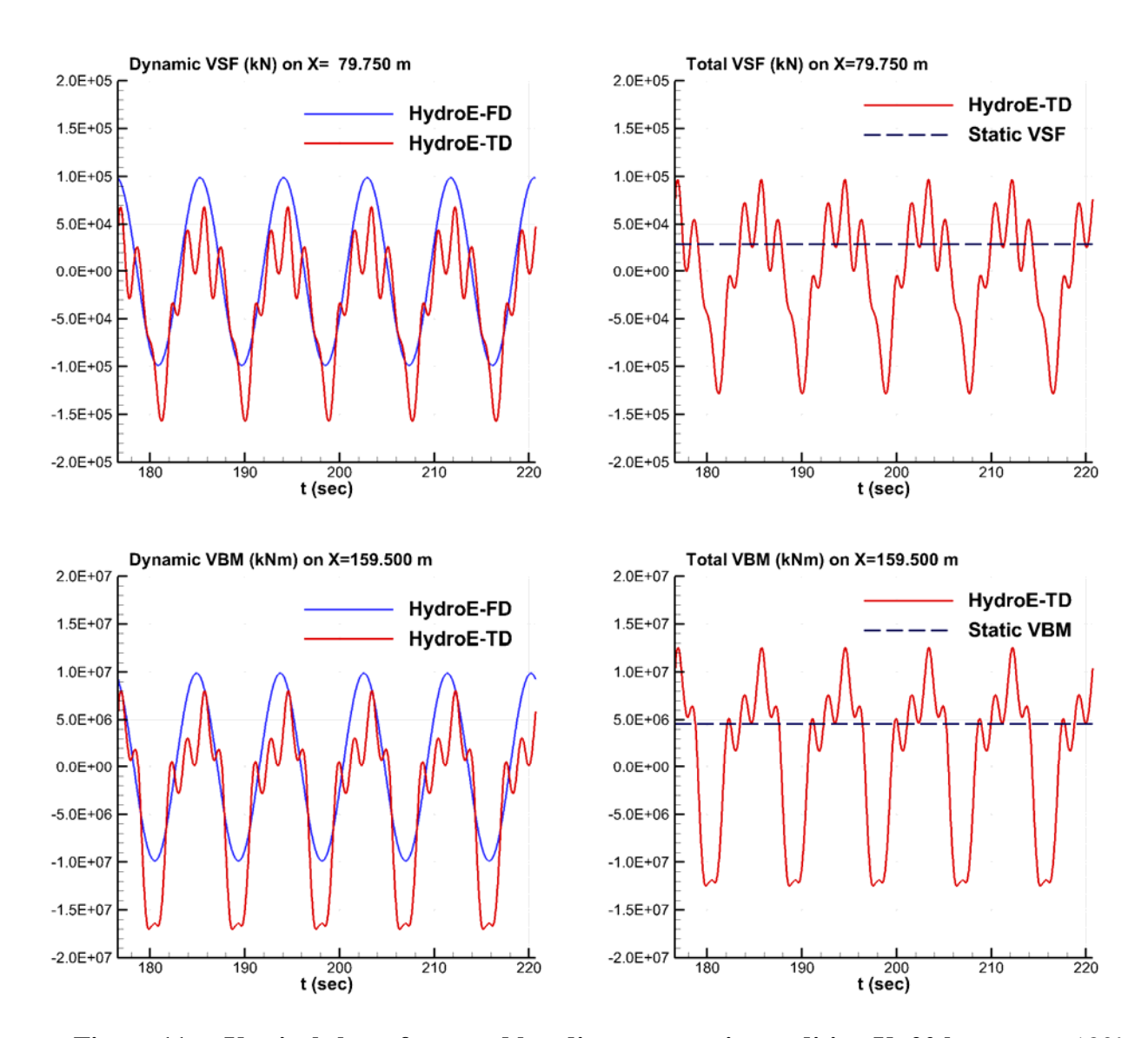


Figure 11: Vertical shear force and bending moment in condition U=20 knots,  $\chi = 180^{\circ}$ ,  $\omega = 0.475$  rad/sec and wave height = 20 meters

The last result presented is the time trace of the first elastic eigenmode, which is an almost pure torque mode for the present ship model, shown in the left of Figure 12, and the time trace of torque load on the mid-ship section. The amplitude of the first elastic mode predicted by the time domain model is smaller than that predicted by the frequency domain, but the torque load predicted by both

methods are almost the same due to the effect of the intermittent and nonlinear pressure correction in the time domain approach.

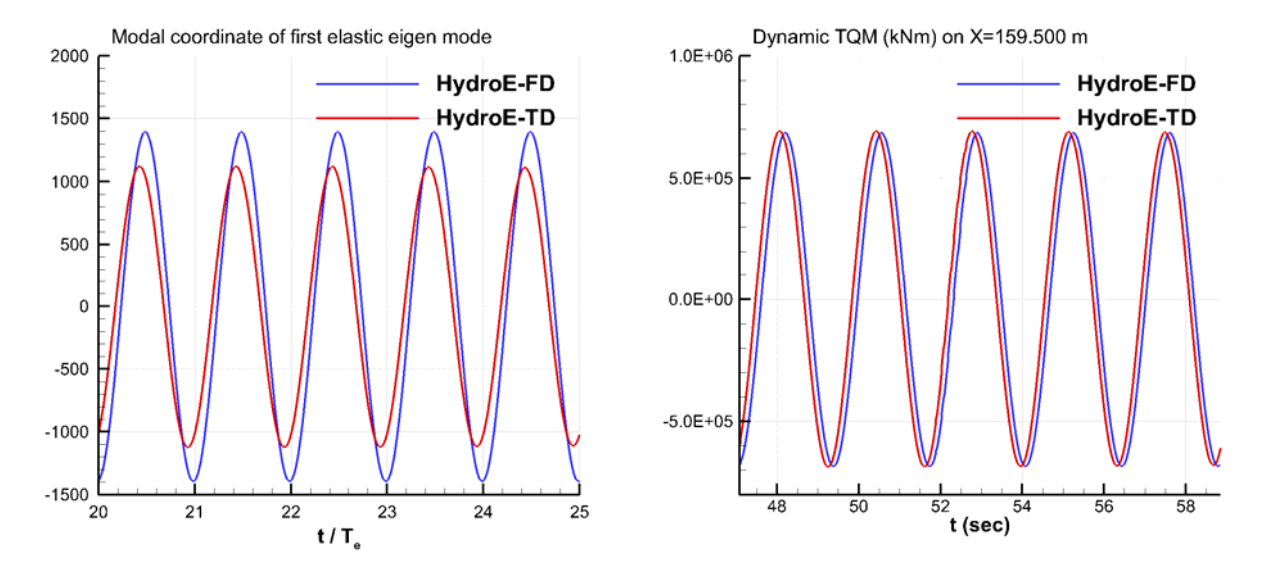


Figure 12: Time trace of first elastic eigenmode amplitude and dynamic torque at mid-ship in condition U=20 knots,  $\chi=150^{\circ}$ ,  $\omega=1.250$  rad/sec (resonant frequency of the 1<sup>st</sup> (torque only) mode) and wave height = 2.82 meters

#### **Conclusions**

The theory of hydroelasticity is outlined for both the linear frequency domain approach and non-linear time domain approach. Results of a container ship of 320 meters in length are used to demonstrate the improvement for hydrodynamic analysis going from rigid-body to elastic body and from frequency domain to time domain. Those results also prove the importance of considering the application of hydroelastic analysis for assessment of ships or structures where structural vibration plays a dominant role.

The authors would like to gratefully acknowledge the support of many colleagues in Lloyd's Register for their contributions to this work. The authors also wish acknowledge support from the Lloyd's Register Global Technology Centre in Southampton, UK, and the Lloyd's Register Applied Technology Group in Halifax, Canada, to publish this work.

The views expressed in this work are those of the authors alone and do not necessarily represent the policy of Lloyd's Register or any of its affiliates or subsidiaries.

#### References

Bishop, R.E.D. and Price, W.G. (1979): Hydroelasticity of Ships, Cambridge University Press.

Wu, Y. (1984): Hydroelasticity of Floating Bodies, Ph.D. Thesis, Brunel Univ., UK

Wang, D. (1996): Three-Dimensional Hydroelastic Analysis of Ships in Time Domain, Ph.D. Thesis, China Ship Scientific Research Centre, China